Research Article | Vol. 25, No. 21 | 16 Oct 2017 | OPTICS EXPRESS 25267
Optics EXPRESS

ENVILAB: Measuring phytoplankton in-vivo absorption and scattering properties under tunable environmental conditions

ANNA GÖRITZ,[1,2,*] STEFAN VON HOESSLIN,[2,3] FELIX HUNDHAUSEN,[2,4] AND PETER GEGE[2]

[1]*Technical University of Munich (TUM), Department of Civil, Geo and Environmental Engineering, Chair of Remote Sensing Technology, Arcisstr. 21, D-80333 München, Germany*
[2]*Remote Sensing Technology Institute, German Aerospace Center (DLR), Münchener Str. 20, Oberpfaffenhofen, D-82234 Weßling, Germany*
[3]*Currently with MTU Aero Engines AG, Dachauer Straße 665, 80995 München, Germany*
[4]*Currently with the Institute for Anthropomatics and Robotics, Karlsruhe Institute of Technology (KIT), Adenauerring 2, D-76131 Karlsruhe, Germany*
**anna.goeritz@tum.de*

Abstract: Optical remote sensing of phytoplankton draws on distinctive spectral features which can vary with both species and environmental conditions. Here, we present a set-up (ENVILAB) for growing phytoplankton under well-defined light, temperature and nutrient conditions. The custom-built light source enables creation of light with spectral composition similar to natural aquatic environments. Spectral tuning allows for light quality studies. Attenuation is monitored with a spectrometer in transmission mode. In combination with automated spectrophotometer and fluorimeter measurements, absorption and excitation-emission-fluorescence spectra are recorded. The set-up opens the door for systematic studies on phytoplankton optical properties and physiology.

OCIS codes: (120.0120) Instrumentation, measurement, and metrology; (280.0280) Remote sensing and sensors; (300.0300) Spectroscopy; (170.6280) Spectroscopy, fluorescence and luminescence; (010.0010) Atmospheric and oceanic optics.

References and links

1. P. Falkowski, "Ocean Science: The power of plankton," Nature **483**(7387), S17–S20 (2012).
2. P. G. Falkowski, "The role of phytoplankton photosynthesis in global biogeochemical cycles," Photosynth. Res. **39**(3), 235–258 (1994).
3. S. Sathyendranath, J. Aiken, S. Alvain, R. Barlow, H. Bouman, A. Bracher, R. Brewin, A. Bricaud, C. W. Brown, A. M. Ciotti, L. A. Clementson, S. E. Craig, E. Devred, N. Hardman-Mountford, T. Hirata, C. Hu, T. S. Kostadinov, S. Lavender, H. Loisel, T. S. Moore, J. Morales, C. B. Mouw, A. Nair, D. Raitsos, C. Roesler, J. D. Shutler, H. M. Sosik, I. Soto, V. Stuart, A. Subramaniam, and J. Uitz, "Phytoplankton functional types from space," in *Reports of the International Ocean Colour Coordinating Group* (IOCCG, 2014).
4. I. Chorus and J. Bertram, "Toxic cyanobacteria in water: a guide to their public health consequences, monitoring and management," E & FN Spon on behalf of the World Health Organization (1999).
5. L. H. Pettersson and D. Pozdnyakov, *Monitoring of Harmful Algal Bloom* (Springer Science & Business Media, 2013).
6. H. J. Gons, M. T. Auer, and S. W. Effler, "Meris satellite chlorophyll mapping of oligotrophic and eutrophic waters in the laurentian great lakes," Remote Sens. Environ. **112**(11), 4098–4106 (2008).
7. L. Li and K. Song, "Chapter 8 - Bio-optical modeling of phycocyanin," in *Bio-optical Modeling and Remote Sensing of Inland Waters*, D. R. Mishra, I. Ogashawara, and A. A. Gitelson, eds. (Elsevier, 2017), pp. 233 – 262.
8. M.-F. Racault, C. L. Quéré, E. Buitenhuis, S. Sathyendranath, and T. Platt, "Phytoplankton phenology in the global ocean," Ecol. Indic. **14**(1), 152–163 (2012).
9. A. G. Dekker, "Detection of optical water quality parameters for eutrophic waters by high resolution remote sensing," Ph.D. thesis (1993).
10. S. G. H. Simis, S. W. M. Peters, and H. J. Gons, "Remote sensing of the cyanobacterial pigment phycocyanin in turbid inland water," Limnol. Oceanogr. **50**(1), 237–245 (2005).
11. L. Li, L. Li, and K. Song, "Remote sensing of freshwater cyanobacteria: An extended IOP inversion model of inland waters (IIMIW) for partitioning absorption coefficient and estimating phycocyanin," Remote Sens. Environ. **157**, 9–23 (2015).

#303126 https://doi.org/10.1364/OE.25.025267
Journal © 2017 Received 21 Jul 2017; revised 1 Sep 2017; accepted 3 Sep 2017; published 4 Oct 2017

Optics EXPRESS

12. N. Tandeau de Marsac, "Occurrence and nature of chromatic adaptation in cyanobacteria," J. Bacteriol. **130**(1), 82–91 (1977).
13. D. Stramski and A. Morel, "Optical properties of photosynthetic picoplankton in different physiological states as affected by growth irradiance," Deep Sea Res. Part A **37**(2), 245–266 (1990).
14. R. MacColl, "Cyanobacterial phycobilisomes," J. Struct. Biol. **124**(2-3), 311–334 (1998).
15. V. A. Lutz, S. Sathyendranath, E. J. H. Head, and W. K. W. Li, "Changes in the in vivo absorption and fluorescence excitation spectra with growth irradiance in three species of phytoplankton," J. Plankton Res. **23**(6), 555–569 (2001).
16. M. Stomp, J. Huisman, F. De Jongh, A. J. Veraart, D. Gerla, M. Rijkeboer, B. W. Ibelings, U. I. Wollenzien, and L. J. Stal, "Adaptive divergence in pigment composition promotes phytoplankton biodiversity," Nature **432**(7013), 104–107 (2004).
17. R. L. Carneiro, M. E. V. dos Santos, A. B. F. Pacheco, and S. M. F. O. Azevedo, "Effects of light intensity and light quality on growth and circadian rhythm of saxitoxins production in cylindrospermopsis raciborskii (cyanobacteria)," J. Plankton Res. **31**(5), 481–488 (2009).
18. H. Xi, M. Hieronymi, R. Röttgers, H. Krasemann, and Z. Qiu, "Hyperspectral differentiation of phytoplankton taxonomic groups: A comparison between using remote sensing reflectance and absorption spectra," Remote Sens. **7**(11), 14781–14805 (2015).
19. T. Parkin and T. Brock, "The effects of light quality on the growth of phototrophic bacteria in lakes," Arch. Microbiol. **125**(1-2), 19–27 (1980).
20. N. Korbee, F. L. Figueroa, and J. Aguilera, "Effect of light quality on the accumulation of photosynthetic pigments, proteins and mycosporine-like amino acids in the red alga porphyra leucosticta (bangiales, rhodophyta)," J. Photochem. Photobiol. B **80**(2), 71–78 (2005).
21. L. Nedbal, M. Trtílek, J. Cervený, O. Komárek, and H. B. Pakrasi, "A photobioreactor system for precision cultivation of photoautotrophic microorganisms and for high-content analysis of suspension dynamics," Biotechnol. Bioeng. **100**(5), 902–910 (2008).
22. C. L. Teo, M. Atta, A. Bukhari, M. Taisir, A. M. Yusuf, and A. Idris, "Enhancing growth and lipid production of marine microalgae for biodiesel production via the use of different LED wavelengths," Bioresour. Technol. **162**, 38–44 (2014).
23. C.-Y. Chen, K.-L. Yeh, R. Aisyah, D.-J. Lee, and J.-S. Chang, "Cultivation, photobioreactor design and harvesting of microalgae for biodiesel production: A critical review," Bioresour. Technol. **102**(1), 71–81 (2011).
24. T. Zavrel, M. A. Sinetova, D. Búzová, P. Literáková, and J. Cervený, "Characterization of a model cyanobacterium synechocystis sp. PCC 6803 autotrophic growth in a flat-panel photobioreactor," Eng. Life Sci. **15**(1), 122–132 (2015).
25. S. von Hößlin, "Development and validation of an automated photobioreactor system for measuring absorption and fluorescence of phytoplankton" Master's thesis, Technische Universität München (2015).
26. S. Muthu, F. J. P. Schuurmans, and M. D. Pashley, "Red, green, and blue LEDs for white light illumination," IEEE J. Sel. Top. Quantum Electron. **8**(2), 333–338 (2002).
27. G. P. E. Steven, W. Brown, and C. Santana, "Development of a tunable LED-based colorimetric source," J. Res. Nat. Inst. Stand. Technol. **107** (2002).
28. K. Fujiwara and A. Yano, "Controllable spectrum artificial sunlight source system using LEDs with 32 different peak wavelengths of 385-910 nm," Bioelectromagnetics **32**(3), 243–252 (2011).
29. D. Kolberg, F. Schubert, N. Lontke, A. Zwigart, and D. Spinner, "Development of tunable close match LED solar simulator with extended spectral range to UV and IRm," Energy Procedia **8**, 100–105 (2011).
30. A. M. Bazzi, Z. Klein, M. Sweeney, K. P. Kroeger, P. S. Shenoy, and P. T. Krein, "Solid-state solar simulator," IEEE Trans. Ind. Appl. **48**(4), 1195–1202 (2012).
31. K. J. Linden, W. R. Neal, and H. B. Serreze, "Adjustable spectrum LED solar simulator," (2014).
32. P. Lu, H. Yang, Y. Pei, J. Li, B. Xue, J. Wang, and J. Li, "Generation of solar spectrum by using LED," (2016).
33. G. Zaid, S.-N. Park, S. Park, and D.-H. Lee, "Differential spectral responsivity measurement of photovoltaic detectors with a light-emitting-diode-based integrating sphere source," Appl. Opt. **49**(35), 6772–6783 (2010).
34. J.-M. Hirvonen, T. Poikonen, A. Vaskuri, P. Kärhä, and E. Ikonen, "Spectrally adjustable quasi-monochromatic radiance source based on LEDs and its application for measuring spectral responsivity of a luminance meter," Meas. Sci. Technol. **24**(11), 115201 (2013).
35. Sinus 220 from Wavelabs Solar Metrology Systems GmbH, Freiburg, Germany, http://wavelabs.de/wp-content/uploads/Brochure_Wavelabs.pdf (accessed on 31st of August 2017).
36. Ecocell from Ecoprogetti Srl, Padova, Italy, https://ecoprogetti.com/Catalogue2016.pdf (accessed on 31st of August 2017).
37. LEDSim, ^{TM} from Aescusoft GmbH, Freiburg, Germany, http://www.aescusoft.com/sites/default/files/public/aes_ledsim_si.pdf (accessed on 31st of August 2017).
38. F. Hundhausen, "Aufbau, Charakterisierung und Ansteuerung eines Beleuchtungs-Moduls zur Simulation variabler Unterwasser-Lichtspektren unter Verwendung von Hochleistungs-Leuchtdioden" Bachelor thesis, Hochschule Esslingen (2015).
39. P. Gege, "Analytic model for the direct and diffuse components of downwelling spectral irradiance in water," Appl. Opt. **51**(9), 1407–1419 (2012).
40. P. Gege, Software WASI, version 4, http://www.ioccg.org/data/software.html (accessed on 17th of July 2017).

Optics EXPRESS

41. Axenic Synechocystis sp. PCC 6803, Pasteur Culture Collection of Cyanobacteria (PCC), Catalogue information available online: https://brclims.pasteur.fr/crbip_catalogue/faces/resultatrecherche.xhtml (accessed on 17th of july 2017).
42. Y. Yu, L. You, D. Liu, W. Hollinshead, Y. J. Tang, and F. Zhang, "Development of Synechocystis sp. PCC 6803 as a phototrophic cell factory," Mar. Drugs **11**(8), 2894–2916 (2013).
43. H. Xu, D. Vavilin, and W. Vermaas, "Chlorophyll b can serve as the major pigment in functional photosystem II complexes of cyanobacteria," Proc. Natl. Acad. Sci. U.S.A. **98**(24), 14168–14173 (2001).
44. G. Johnsen, A. Bricaud, N. Nelson, B. B. Preélin, and R. R. Bidigare, *Phytoplankton Pigments: Characterization, Chemotaxonomy, and Application in Oceanography* (Cambridge University, 2011).
45. R. Rippka, J. Deruelles, J. B. Waterbury, M. Herdman, and R. Y. Stanier, "Generic assignments, strain histories and properties of pure cultures of cyanobacteria," Microbiology **111**(1), 1–61 (1979).
46. J. Lakowicz, *Principles of Fluorescence Spectroscopy* (Springer US, 2013).
47. C. D. Mobley, *Light and Water: Radiative Transfer in Natural Waters* (Academic, 1994).
48. S. G. H. Simis, Y. Huot, M. Babin, J. Seppälä, and L. Metsamaa, "Optimization of variable fluorescence measurements of phytoplankton communities with cyanobacteria," Photosynth. Res. **112**(1), 13–30 (2012).
49. P. Gege, "Chapter 2 - Radiative Transfer Theory for Inland Waters," in *Bio-optical Modeling and Remote Sensing of Inland Water*s (Elsevier, 2017).
50. M. Stomp, J. Huisman, L. Vörös, F. R. Pick, M. Laamanen, T. Haverkamp, and L. J. Stal, "Colourful coexistence of red and green picocyanobacteria in lakes and seas," Ecol. Lett. **10**(4), 290–298 (2007).

1. Introduction

Phytoplankton forms the basis of the aquatic food web and plays a fundamental role in biogeochemical cycles in the ocean [1–3]. Certain phytoplankton species such as *Microcystis* are potential toxin producers and their monitoring is of interest to many stakeholders such as environment agencies, aquaculture or water resource managers [4,5].

Due to its pigmentation and its specific scattering properties, phytoplankton can be detected in remotely sensed data from satellite, air- and shipborne as well as from ground based measurements. Optical signatures such as absorption and fluorescence by chlorophyll-*a* or specific backscattering properties serve for identification and separation from other water constituents in reflectance signals. These signatures are used to infer phytoplankton concentration and its spatial distribution on both local and global scales, e.g. [6–8]. In case of cyanobacteria, remote sensing algorithms often exploit spectral features originating from additional pigments in light harvesting complexes such as from phycocyanin [9–11]. Several studies on phytoplankton suggest that pigment composition can change not only from species to species but also with environmental conditions [12–16]. For remote sensing modelling, it is crucial to understand this variability in the inherent optical properties (IOPs), since it affects accuracy and sensitivity of retrieval algorithms. Systematic laboratory studies on phytoplankton *in-vivo* absorption and scattering characteristics under controlled environmental conditions are rare. Further, they are usually performed under so called day-light conditions (e.g [17,18].). For this purpose, a light source (often a fluorescent tube) is used that provides continuous radiation in the 400 nm to 700 nm wavelengths range (photosynthetically active radiation – PAR). Assuring a certain PAR emission with day-light lamps helps to create stable and reproducible culturing conditions. However, the actual spectral composition (e.g., uneven spectral distribution and high distinctive emission peaks for fluorescent lamps), and how it compares to light that phytoplankton is exposed to in its aquatic environments is usually neglected. A few studies focus on the impact of spectral composition of light on phytoplankton and algae, but for this purpose usually lamps with color filters or a few individual light emitting diodes (LEDs) are chosen [19–21].

Recently, especially in the context of bio-fuel and biotechnology applications, there have been many studies on light influencing growth behavior of bacteria and algae. The motivation for these studies often is to increase growth rates and lipid production. Light sources for culturing are optimized towards yielding highest growth rates, lipid and large-scale production rather than to resemble natural conditions [22–24]. Therefore, culturing assemblies designed for bio-fuel applications usually do not allow for an investigation of phytoplankton growth under natural light conditions.

Optics EXPRESS

In the present contribution, a novel set-up for optical studies on phytoplankton is presented. It allows for controlled phytoplankton growth and serves as a stage for experimental investigation of changes in phytoplankton physiology in response to varying light field, nutrient or temperature conditions. With the help of a tunable multispectral light source, phytoplankton can be grown under a broad variety of artificial and natural light conditions with respect to intensity and spectral composition. Automated spectrometric measurements allow to analyze absorption and scattering characteristics.

After an introduction to the set-up design with focus on its individual components and the spectrometric data that is recorded, the functional range is demonstrated by growth and dilution of a cyanobacteria culture.

2. Design and Realization of the ENVILAB Set-up

2.1 System Concept

Phytoplankton is grown in a photo-bioreactor under light that is provided by a custom-built multispectral LED light source tunable in both spectral composition and intensity. Growth is monitored by a spectrometer that measures spectral transmission and thus attenuation of light through the reactor chamber. Via an automated peristaltic pumping system, the growth chamber is linked with a benchtop fluorimeter and spectrophotometer with an integrating sphere for recording high precision fluorescence and absorption spectra. An estimate on scattering properties can be obtained by subtracting absorption from attenuation spectra. Stirring and automated dilution of the culture with nutrient medium allows long term experiments and studies at fixed concentration ranges. Tubes for sample transportation can be cleaned with a cleansing liquid in between or after measurements. Specifically designed software allows for live monitoring of growth parameters such as the optical depth. A sketch of the experimental set-up is depicted in Fig. 1.

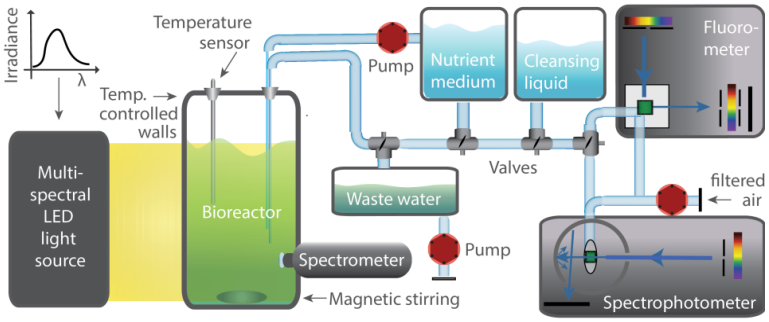

Fig. 1. Schematic sketch of the measurement set-up (modified from [25]).

2.2 Tunable LED-light Source for Spectral Light Field Simulation

Tunable LED-based light simulators, as described in the literature, are realized in a variety of designs for applications such as color rendering [26,27], solar spectrum simulation [28–32] and responsivity measurements [33,34]. The respective light sources differ in number, types and combination of LEDs, as well as in their electronic control and additional optical components. Accordingly, they exhibit different characteristics in terms of spectral matching, illumination area and irradiance intensities. In photovoltaics (PV), commercial set-ups exist that are optimized towards accurate and stable reproduction of solar irradiance for characterization of PV cells [35–37]. For this purpose, assemblies with LEDs of typically around 20 different peak wavelengths are used to provide light in the visible and in parts of the ultraviolet and infrared. Illumination areas are designed to cover standard PV cell sizes. For biological studies, Fujiwara and Yano present a set-up consisting of 547 LEDs with 32 different peak wavelengths [28]. This light source provides high spectral flexibility in the 385

Optics EXPRESS

- 910 nm wavelength range illuminating an area of about 7cm^2. Linden et al. report on a tunable solar simulator with modular design for illumination of different sizes and shapes, but with less spectral matching flexibility in the visible (LEDs with 23 different peak wavelengths for cover the 350 to 1100 nm wavelength range) [31].

Here, we present a tunable, multispectral LED light source which is specifically designed for phytoplankton studies in a photobioreactor [38]. Special attention was paid to spectral flexibility and the resemblance of the obtained irradiance spectra to spectra found in aquatic environments. In addition to sun position and metrological conditions, spectral composition of underwater irradiance changes with depth, bottom type and vegetation, and water constituent concentrations. In order to simulate a variety of irradiance scenarios in the photosynthetically active radiation range of 400 nm to 700 nm, multiple LEDs were selected according to their high intensities, spectral peak position and bandwidths: Intensities are high enough to match (in sum) maximum spectral irradiance below the water surface. The latter was simulated using the Water Color Simulator (WASI) software (at a sun zenith angle of 0° and a sensor depth of 0 m) [26,27]. Actual bandwidths of LEDs span around 13 to 38 nm (FWHM), with the exception of two types of phosphor coated broad band LEDs which were added to fill the gap between 530 nm and 600 nm at which LEDs are difficult to find. Position of emission peaks are chosen to assure both spectral continuity and flexibility which is needed to match target spectra [39,40].

All LEDs (72 with 24 different peak wavelengths) are placed on Aluminium plates which together are arranged in arrays (see Fig. 2(a)). These arrays are mounted on heat dissipaters in such a way, that individual LED plates remain replaceable. The temperature of the heat sink is monitored; fans attached provide additional cooling in case the temperature rises above a given threshold (typically 25 °C).

In order to assure homogeneity of radiance across the illuminated area, the LED arrays are mounted into a mirror foil covered tube of rectangular shape (see Fig. 2(b)). Reflection at surface walls together with a diffuser plate (*PLEXIGLAS® Satinice)* at the tube's exit, restrict inhomogeneity to less than 10% within the illuminated area of 10 cm × 20 cm.

Spectral characteristics of each LED (mounted in module) were determined at lab conditions with a spectrometer (*CARL ZEISS MCS 500,* 350-1021 nm, 0.8° field-of-view) at LED current intensity of 350 mA. The calibrated spectra are stored in a database. This database forms the spectral library used to determine pulse width modulation (PWM) duties for individual LEDs in designated control software. Via a graphical user interface, target spectra can be loaded. These target spectra are either artificially composed, measured or simulated irradiance spectra that cover the 400-800 nm wavelength region and which are to be reproduced by the light source. PWM duties of the corresponding LEDs are set by the control software using a least-square-fit between the target spectrum and the sum of individual LED spectra. In a cycling mode, user defined target spectra can be varied over time. This way, day and night cycles, spectral shifts or sudden changes in illumination can be simulated. A summary on technical details of the light source can be found in Table 1.

Optics EXPRESS

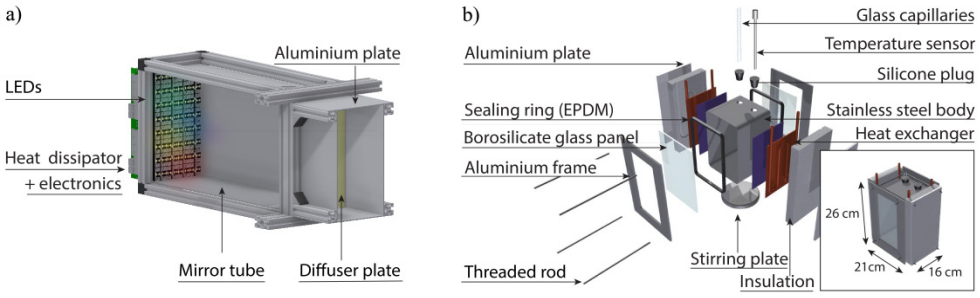

Fig. 2. (a) Schematic sketch of LED light source; (b) Scheme of bioreactor assembly in explosion view; area of glass windows match illumination area of multispectral light source (modified from [25,38]).

Table 1. Technical specifications of the LED light source.

LEDs (total number)	72 LEDs of 24 different peak wavelengths.
Peak wavelength / FWHM [nm]	403/15, 421/16, 427/17, 433/19, 445/20, 467/25, 470/25, 472/25, 494/29, 506/32, 521/38, 522/37, 561/101, 594/18, 603/80, 621/18, 636/19, 657/20, 676/22, 684/26, 687/23, 705/25, 727/32, white/139.
Max. power/irradiance	~8 W on an area of 10 cm × 20 cm.
Hardware control	Custom designed circuit board with 32 independent PWM-controlled LED drivers (350 mA LED string current); setting of PWM duty via an I2C interface (12 bits resolution, frequencies up to 1526 Hz); temperature monitoring ICs and PWM-controlled fans.

2.3 Photobioreactor

Individual components of the photobioreactor [25] were designed while having both the microbiological and optical requirements in mind: In order to minimize contamination for microbiological studies on phytoplankton samples, all parts can be disassembled, cleaned and sterilized in an autoclave. In addition, electro-polished stainless steel of 2 mm thickness as frame material hinders deposition of phytoplankton on the inner walls. To fulfill optical demands, Borosilicate windows were chosen that provide over 90% transmission for light in the 390 to 750 nm wavelength range.

Figure 2(b) shows a sketch of the photobioreactor assembly in explosion view. The base area was matched to a magnetic stirrer plate of 12.5 cm diameter. This way, velocity controlled mixing within the reactor is possible by inserting a Polytetrafluorethylene (PTFE) coated stirrer. The reactor's inner dimensions comprise a volume of about 3.5 l of sample liquid which can be inserted and extracted via glass tubes that are connected to flexible tubes. Liquids in the tubing connection are transported with a four-channel peristaltic pump. Fluid pathways are controlled by magnetic pinch valves which open when voltage is applied. These valves are triggered by a microcontroller. Inside the incubation chamber, temperature is monitored with a digital temperature sensor in a steel casing. On the two sides of the chamber's frame, custom-built copper plates provide heat-exchange to a liquid that can be heated or cooled by a thermostat. Insulation of the chamber body from ambient conditions assures additional temperature stability.

Software with Graphical User Interface allows creation of a timeline that includes all relevant pumping and measurement steps. A cycling function can be activated for repetitive experiments. Once the involved volumes are defined, the software visualizes current liquid levels and allows for live temperature and optical growth monitoring.

Optics EXPRESS

2.4 Spectrometric Monitoring

The ENVILAB set-up provides a two-step spectral monitoring making use of a miniaturized spectrometer (*FREEDOM VIS FSV-305*, Ibsen Photonics Inc., Denmark) for transmission measurements, and of two bench-top instruments for recording absorption and fluorescence spectra (*LAMBDA®1050,* PerkinElmer Inc., U.S., and *FLUOROMAX®4*, HORIBA Scientific, Japan). The transmission of light through the sample liquid is measured regularly using the *FREEDOM VIS* spectrometer. This way, the decrease in transmission is monitored and thus, by application of Beer–Lambert's law, the growth rate is recorded. For high precision measurements with minimal scattering influence, samples are pumped into a flow-through quartz cuvette, which is mounted inside of the 150 mm diameter integrating sphere of the double beam spectrophotometer. In parallel, the fluorescence spectrum at a selected excitation wavelength or a full excitation and emission spectrum is recorded. Emitted light is detected under 90 degrees to the excitation light beam. Fluorescence measurements are normalized to excitation light intensities as measured with the instrument's reference detector, and manufacturer's correction factors are applied. After each measurement cycle, the respective cuvettes are automatically emptied into a waste collection flask and both tubes and cuvettes are flushed with a cleansing liquid.

3. Functional Tests and Discussion

3.1 Irradiance Simulation and Temperature Control

Motivation for designing the LED light source was to reproduce both artificial and natural irradiance spectra. Figure 3 illustrates target spectra resembling for three different irradiance scenarios: (a) at water surface, (b) in water rich of colored dissolved organic matter (CDOM) at 1 m depth and (c) at 3 m water depth. All spectra were simulated with WASI (for a sun zenith angle of 40 °, a total suspended matter concentration of 1.5 mg l^{-1}, an absorption of CDOM at 440 nm of 0.2 m^{-1} with a slope of S_{CDOM} = 0.014 nm^{-1} and a phytoplankton concentration of 3 µg l^{-1}). Black lines represent simulated spectra and colored lines individual LEDs, while grey diamonds reflect the total LED irradiance.

In Fig. 3, maximum relative deviation (per nm) from target irradiance of 54% in case (a) and 34-35% in case (b) and (c) can be observed, with an average deviation of 14%, 6% and 8%, respectively. This is caused by spectral overlap of the emission peaks. Especially if lower water depths are to be simulated, higher average deviation from target spectra will be observed. The reason for this is that, in larger depth, more light gets absorbed by the water itself, leading to pronounced spectral features around 600 nm. The coverage of the corresponding wavelength range with broad band LEDs does not allow for proper reproduction of these spectral features in the irradiance spectra. At the time when the light source was built, no suitable LEDs were available to cover the 550 to 600 nm wavelength regions.

Despite these drawbacks, the light source provides much more flexibility in resembling natural irradiance spectra than conventional light sources. No additional filters are necessary to avoid unwanted peaks. In addition, relative intensities of "overshoots" are much smaller compared to fluorescent tubes, where distinctive peaks of chemical compounds affect the emission spectrum.

Optics EXPRESS

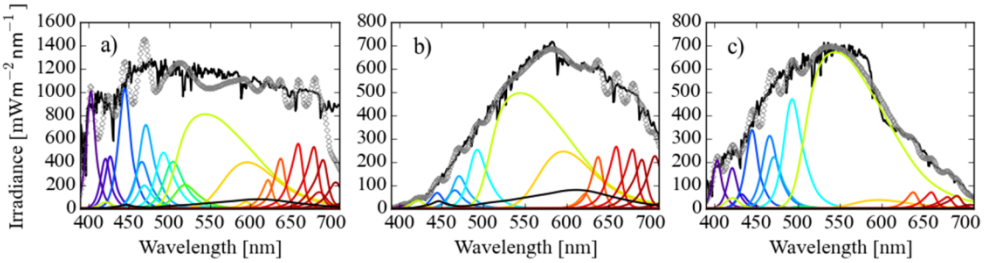

Fig. 3. Calculated (black solid line) and simulated (grey circles) downwelling irradiance spectra for different ambient light scenarios under a sun zenith angle of 40°: (a) at water surface (sensor depth = 0 m), (b) with high CDOM concentration at 1 m depth (a_{CDOM} = 2 m^{-1}) and (c) at 3 m water depth. Colored lines reflect individual LED spectra.

Temperature stability inside the photobioreactor was tested in the laboratory at room temperature. For this purpose, 1.2 l and 3 l of purified water was cooled and heated via the heat exchanger using the thermostat which was to set values in the range of 1 to 40 °C. Tests confirmed stable temperature conditions in the range of 2.6 to 39.1 ± 0.1 °C with maximum deviation of 3°C for most extreme temperatures and depending on the filling level. Tests confirmed that the ENVILAB enables a variety of studies at temperatures typically found in natural water bodies [25].

3.2 Automated Spectral Measurements and Nutrient Control

First phytoplankton growth tests were performed with *Synechocystis sp*. PCC 6803 [41]. This cyanobacterium is widely studied [42], making it an interesting model organism.

For bioreactor functionality validation, the culture was kept under light with fixed spectral composition. In order to produce an intensity similar to previous culturing conditions, the irradiance spectrum (at 2 m water depth; simulated with *WASI* default parameters) was additionally attenuated by a factor of 10. Light was switched on and off in a day-and-night cycle (14 h/10 h). A baseline measurement with pure nutrient medium was performed before adding the culture.

To validate the growth monitoring ability, transmission of a culture of PCC 6803 bacteria was measured with the *FREEDOM VIS* spectrometer during a period of 6.3 days with a series of 10 spectra every 15 minutes. Dark current measurements were recorded directly before start of the growth experiment and during night phases. The corresponding 3540 extinction spectra are shown in Fig. 4(a). They illustrate the continuous growth during day times which result in an increase in attenuation. The attenuation peaks correspond to phytoplankton pigments. The peak around 436 nm and the peak at around 673 nm can be associated with absorption by chlorophyll pigments. The peak around 620 – 630 nm relates to phycocyanin absorption [43,44].

In order to test automated measurement cycles and nutrient supply, a series of dilution measurements with PCC 6803 (grown under traditional day-light) was recorded. Over 24 hours, a dense culture inside the photobioreactor was stepwise diluted with nutrient medium (BG11 modified from [45]) until noise contribution became too high to acquire meaningful spectra [25]. Figure 4(b) shows the corresponding absorption spectra. The decrease in absorption corresponds to a reduction of cyanobacteria concentration. The absorption decreases linearly over the wavelength range of 300 nm to 700 nm as shown in the inset of Fig. 3(b).

Optics EXPRESS

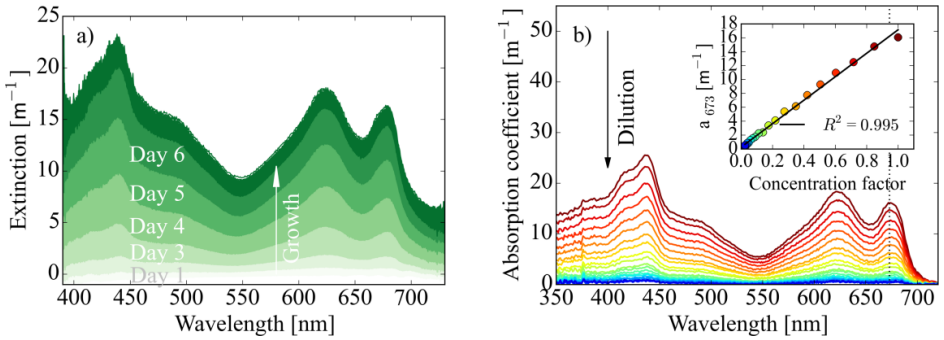

Fig. 4. (a) Growth of *Synechocystis sp*. (PCC 6803) monitored through the reactor windows; transmission was measured ten times during day every 15 minutes over a period of ~6.3 days leading to the depicted 3540 spectra. (b) Absorption spectra during automated dilution of a PCC 6803 culture; inset: corresponding concentration factor vs. absorption at 673 nm.

At each dilution step, excitation-emission spectra were recorded. In order to reduce acquisition time, the wavelength range of interest was split in two: a) with an excitation (λ_{ex}) from 200 – 700 nm and an emission (λ_{em}) from 575 – 800 nm, b) with λ_{ex} from 200 – 540 nm and λ_{em} from 250 – 575 nm. The two EEM (excitation-emission matrices) spectra at every dilution step were automatically recorded right after each other (5 nm wavelength steps, 2 nm bandpass front and exit slit, 0.1 s integration time). After adding the spectra to combined EEMs, the pure nutrient EEM was subtracted. Figure 5(a) illustrates an example of such a blank corrected EEM. High intensities at diagonal values ($\lambda_{ex} = \lambda_{em}$) are due to elastic scattering (Rayleigh) and instrument effects. Also second order effects at doubled emission wavelength ($\lambda_{em} = 2\lambda_{ex}$) can be observed. For further analysis, Rayleigh scattering was masked out, leading to blanks in diagonal matrix values which occur as gaps in the excitation spectrum at 680 nm emission as shown in Fig. 5(b).

EEM spectra show that fluorescence emission maxima were shifted towards longer wavelengths as compared to absorption spectra, which is to be expected for this inelastic scattering process. Fluorescence intensity at 620 nm excitation and 680 nm emission ($f_{430/685}$) decreases linearly with dilution (see inset of Fig. 5(b)). This proves that measurements were not impacted by non-linear effects such as the inner filter effect (i.e. reabsorption of fluorescence photons by the sample) [25,46].

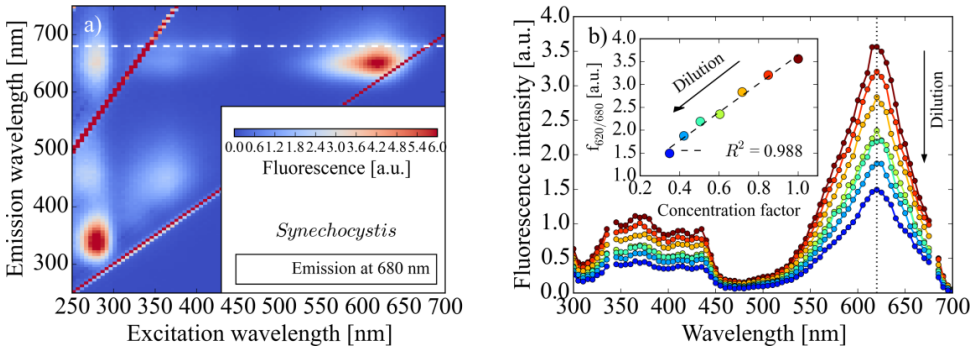

Fig. 5. (a) Excitation-mission spectrum of *Synechocystis sp.* (PCC6803) after blank subtraction. The dashed line indicates the excitation spectrum at 680 nm emission. (b) Excitation spectrum at 680 nm for PCC 6803 at different dilution steps. The inset indicates linear decrease of fluorescence intensity at 620 nm excitation and 680 nm emission with dilution.

Optics EXPRESS

4. Conclusion and Outlook

In this paper, a novel automated spectrometric set-up (ENVILAB) was presented, which enables controlled phytoplankton growth and at the same time allows for the characterization of its bulk attenuation, absorption and fluorescence characteristics. The custom-built, tunable, multispectral LED light source permits systematic studies on phytoplankton under varying light conditions. Consisting of 72 LEDs of 24 different peak wavelengths, irradiance intensities and spectral compositions of the light source are tunable in a wavelength range of about 380 to 700 nm. Maximum irradiance matches that of natural sun close to the water surface (with a zenith angle of 0°). The flexibility of the LED light source for natural light field simulation has been demonstrated on three examples at different underwater conditions. Thus, together with under-water irradiance simulation not only artificial but also under-water light scenarios similar to natural conditions (in terms of spectral composition) can be reproduced. In combination with the time line function, both sudden and slow changes in spectral composition and its impact on phytoplankton growth and optical properties can be studied. Further improvement of the light source should address finer reproduction of spectral feature, especially in the 550 to 600 nm wavelength range.

In the photobioreactor of the ENVILAB, cultures of phytoplankton can be grown under controlled environmental conditions. Temperature stabilization is realized via a heat exchanger which in combination with a thermostat assures temperatures in the range of 2.6 to 39.1 ± 0.1 °C. Currently, no gas exchange is included but additional openings in the steel frame of the bioreactor provide access if future implementation (e.g. of a bubbling system) is desired.

For validation of growth monitoring, *Synechocystis sp.* (PCC 6803) was grown in a stirred culture. Monitoring the LED light through the flat transmission windows using an external miniaturized spectrometer has been proven to be suitable for monitoring of changes in the attenuation of the culture.

Nutrient supply and automated measurement procedures were tested by continuously diluting a *Synechocystis* PCC 6803 culture with nutrient medium. With every automated dilution step, samples were programmed to be withdrawn from the bioreactor via the automated peristaltic pumping system, transported into the photometer and fluorimeter and spectra were recorded. This way, *in-vivo* absorption and fluorescence measurements could be performed externally with minimally invasive sample extraction. Absorption was determined inside an integrating sphere of the photometer, while fluorescence was recorded in a compact steady state fluorimeter which allows for excitation-emission measurements. For fixed concentration range studies, current attenuation of the phytoplankton culture inside the photobioreactor can be measured and the corresponding optical depth values are fed into the automated nutrient dilution programming loop. This loop controls concentration by mixing fresh nutrient medium into the bioreactor until the optical density has reached the desired value.

In summary, ENVILAB provides a novel laboratory environment for systematic studies on phytoplankton physiology and optical properties. Next to attenuation measurements, which give insight into scattering properties, absorption and fluorescence measurements on *in-vivo* samples are collected. This spectral information is highly valuable as it builds the basis for water constituent and pigment discrimination in many applications ranging from remote sensing to optical *in situ* devices [47–49]. Reduction of uncertainties in the IOPs and understanding its natural variability may therefore improve water quality monitoring in the long term [7]. In addition, control and adjustability of environmental factors during phytoplankton growth (such as light and its spectral composition, temperature and nutrient supply), enable experiments in various fields of phytoplankton research such as chromatic adaptation, day-night cycle or niche behavior [13,50].

Optics EXPRESS

Funding

A. Göritz gratefully acknowledges support by the Deutsche Forschungsgemeinschaft (DFG) through the TUM International Graduate School of Science and Engineering (IGSSE) and a TUM Laura-Bassi-Fellowship.

Acknowledgments

The authors would like to thank Christoph Haisch, Michael Seidel and Katrin Zwirglmaier for discussions at an early stage of this project. Further, they want to thank Pia Scherer and Joachim Ruber for support in culture handling and cultivation techniques and Katharina Einberger and Jürgen Wörishofer for technical assistance.